Redox Biology 28 (2020) 101381

Contents lists available at ScienceDirect

Redox Biology

journal homepage: www.elsevier.com/locate/redox

Research Paper

Acetaldehyde induces phosphorylation of dynamin-related protein 1 and mitochondrial dysfunction via elevating intracellular ROS and Ca^{2+} levels

Tingting Yan, Yan Zhao*

Department of Bioengineering, Harbin Institute of Technology, Weihai, 264209, Shandong, China

ARTICLE INFO

Keywords:
Acetaldehyde
Mitochondria
Drp1
Oxidative stress
Ca^{2+}

ABSTRACT

Excessive alcohol consumption impairs brain function and has been associated with an earlier onset of neurodegenerative diseases such as Alzheimer's disease (AD) and Parkinson's disease (PD). Acetaldehyde, the most toxic metabolite of alcohol, has been speculated to mediate the neurotoxicity induced by alcohol abuse. However, the precise mechanisms by which acetaldehyde induces neurotoxicity remain elusive. In this study, it was found that acetaldehyde treatment induced excessive mitochondrial fragmentation, impaired mitochondrial function and caused cytotoxicity in cortical neurons and SH-SY5Y cells. Further analyses showed that acetaldehyde induced the phosphorylation of mitochondrial fission related protein dynamin-related protein 1 (Drp1) at Ser616 and promoted its translocation to mitochondria. The elevation of Drp1 phosphorylation was partly dependent on the reactive oxygen species (ROS)-mediated activation of c-Jun-N-terminal kinase (JNK) and p38 mitogen-activated protein kinase (MAPK), as N-acetyl-L-cysteine (NAC) pretreatment inhibited the activation of JNK and p38 MAPK while attenuating Drp1 phosphorylation in acetaldehyde-treated cells. In addition, acetaldehyde treatment elevated intracellular Ca^{2+} level and activated Ca^{2+}/calmodulin-dependent protein kinase II (CaMKII). Pretreatment of CaMKII inhibitor prevented Drp1 phosphorylation in acetaldehyde-treated cells and ameliorated acetaldehyde-induced cytotoxicity, suggesting that CaMKII was a key effector mediating acetaldehyde-induced Drp1 phosphorylation and mitochondrial dysfunction. Taken together, acetaldehyde induced cytotoxicity by promoting excessive Drp1 phosphorylation and mitochondrial fragmentation. Both ROS and Ca^{2+}-mediated signaling pathways played important roles in acetaldehyde-induced Drp1 phosphorylation. The results also suggested that prevention of oxidative stress by antioxidants might be beneficial for preventing neurotoxicity associated with acetaldehyde and alcohol abuse.

1. Introduction

Mitochondria are vital organelles in eukaryotic cells which play indispensable roles in ATP generation, Ca^{2+} homeostasis and cell survival. Because of the high metabolic demands, neurons are sensitive to the alteration of mitochondrial function [1]. Accumulating evidence has shown that the dysfunction of mitochondria is a prominent and early event in neurodegenerative diseases such as Alzheimer's disease (AD) [3,79]. As highly dynamic organelles, mitochondria constantly divide and fuse with each other. The balance of fission and fusion is critical for maintaining the normal structure and function of mitochondria [5[12]]. Impaired mitochondrial dynamics can result in the accumulation of defective mitochondria and is involved in the pathogenesis of neurodegenerative diseases [4,6,7]. Morphological analyses of neurons from AD patients show that the percentage of mitochondria with intact ultrastructure is significantly lower when compared with the neurons from the age-matched controls [8]. Similarly, the number of fragmented mitochondria with broken ultrastructure is increased in neurons of Tg2576 transgenic AD mouse model overexpressing amyloid precursor protein with “Swedish” mutation [9]. The mitochondria in AD neurons have reduced length possibly resulted from the excessive mitochondrial fission [9,10].

A number of proteins are involved in the regulation of the fission and fusion processes of mitochondria. The fission of mitochondria is mainly driven by a GTPase family member dynamin-related protein 1 (Drp1), which exists as dimers or tetramers in cytoplasm [11,13,14].

Abbreviations: AD, Alzheimer's disease; **ADH**, alcohol dehydrogenase; **ALDH2**, aldehyde dehydrogenase 2; **CaMKII**, Ca^{2+}/calmodulin-dependent protein kinase II; **Drp1**, dynamin-related protein 1; **JNK**, c-Jun-N-terminal kinase; **MAPK**, mitogen-activated protein kinase; **Mfn1**, mitofusin 1; **NAC**, N-acetyl-L-cysteine; **OPA1**, optic atrophy 1; **PD**, Parkinson's disease; **ROS**, reactive oxygen species

* Corresponding author.
E-mail address: zhaoyan@hitwh.edu.cn (Y. Zhao).

https://doi.org/10.1016/j.redox.2019.101381
Received 4 August 2019; Received in revised form 31 October 2019; Accepted 10 November 2019
Available online 11 November 2019

During mitochondrial fission, Drp1 is recruited to the mitochondrial outer membrane where it assembles into larger oligomeric fission complex and evokes the mitochondrial fission by GTP hydrolysis [15,16]. The function of Drp1 is regulated by extensive post-translational modulation, such as phosphorylation, sumoylation and ubiquitination, which may affect the protein stability of Drp1, the localization of Drp1 to mitochondria, or the formation of fission complex at mitochondrial fission sites [15,17–19]. Under various stimuli, Drp1 activity can be altered, resulting in abnormal mitochondrial dynamics and cell injuries. It has been demonstrated that oxidative stress augments the GTPase activity of Drp1 and promotes Drp1-mediated mitochondrial fragmentation and dysfunction [16,20[41]], while inhibition of oxidative stress restores tubular mitochondrial morphology [21]. In addition, elevation of intracellular Ca^{2+} levels and mitochondrial Ca^{2+} uptake are also involved in the modulation of Drp1-mediated mitochondrial fragmentation [22]. The excessive mitochondrial fission resulted from the augmented Drp1 activity may consequently lead to the production of defective mitochondria in neurons, causing neurotoxicity and ultimately promoting the pathological development of neurodegenerative diseases.

It has been demonstrated that chronic alcohol abuse causes brain damages and perhaps accelerates the onset and development of neurodegenerative diseases such as AD and Parkinson's disease (PD) [23,24]. Acetaldehyde, the most toxic metabolite of alcohol, has been speculated to play important role in mediating the neurotoxicity induced by alcohol abuse. Acetaldehyde is mainly generated in liver from ethanol by alcohol dehydrogenase (ADH) after absorption. Catalase and cytochrome p450 2E1 are additional enzymes which are critical for the local formation of acetaldehyde in the brain [25]. The major enzyme responsible for the detoxification and metabolism of acetaldehyde is aldehyde dehydrogenase 2 (ALDH2). Excessive alcohol consumption can lead to higher blood concentration of acetaldehyde especially in individuals with defective ALDH2 [26]. The generation and accumulation of acetaldehyde by local metabolism in brain may mediate the brain tissue damage and the cognitive dysfunction induced by chronic excessive consumption of alcohol. Oxidative stress has been implicated in acetaldehyde-induced cytotoxicity and tissue damages [27–29]. Studies have shown that excess acetaldehyde leads to increased expression of NADPH oxidase 2 (NOX2) subunits and enhanced NOX activity, which play important role in acetaldehyde-induced mitochondrial reactive oxygen species (ROS) generation [30,31]. It has been demonstrated that acetaldehyde induces ROS overproduction and impairs mitochondrial function, causing apoptosis and cytotoxicity of neuronal cells [29,[31]32,]. However, the precise mechanisms by which acetaldehyde induces mitochondrial dysfunction and neurotoxicity are still unclear. Here we found that acetaldehyde induced mitochondrial fragmentation and dysfunction in SH-SY5Y cells by promoting the phosphorylation and mitochondrial translocation of Drp1. Further analyses showed that the increased production of ROS and the elevation of intracellular Ca^{2+} were critical for acetaldehyde-induced Drp1 phosphorylation and mitochondrial dysfunction.

2. Materials and Methods

2.1. Materials

Fetal bovine serum (FBS), streptomycin, penicillin, Dulbecco's modified Eagle's medium (DMEM), trypsin, beta tubulin antibody, MitoTracker™ Green FM and MitoSOX™ Red mitochondrial superoxide indicator were purchased from Thermo Fisher Scientific (Rockford, USA). Acetaldehyde, crystal violet and N-acetyl-L-cysteine (NAC) were purchased from Sangon Biotech (Shanghai, China). 3-(4,5-dimethylthiazol-2-yl)-2,5-diphenyl tetrazolium bromide (MTT) assay kit was purchased from Wanleibio (Shenyang, China). BCA protein assay kit, ATP assay kit, mitochondrial membrane potential ($\Delta\Psi$) assay kit, mitochondria isolation kit, Fluo-3 AM, dimethyl sulfoxide (DMSO), BeyoECL plus Western blotting detection system, HRP-labeled donkey anti-goat IgG (H + L), HRP-labeled goat anti-mouse IgG (H + L) and HRP-labeled goat anti-rabbit IgG (H + L) were purchased from Beyotime Institute of Biotechnology (Haimen, China). KN-93 phosphate was purchased from Selleck Chemicals (Houston, USA). BAPTA-AM was purchased from TargetMol (Boston, USA). 2′, 7′-dichlorodihydrofluorescein diacetate (DCFH-DA) was purchased from Sigma Chemical (St. Louis, MO, USA). Phospho-Drp1 (p-Drp1) (Ser616) antibody, Drp1 antibody, phospho-JNK (p-JNK) (Thr183/Tyr185) antibody, JNK antibody, phospho-p38 MAPK (p-p38 MAPK) (Thr180/Tyr182) antibody, p38 MAPK antibody, phospho-CaMKII (p-CaMKII) (Thr286) antibody and CaMKII antibody were purchased from Cell Signaling Technology (Danvers, USA). OPA1 (D-9) antibody, Mfn1 (D-10) antibody and Tim23 (H-8) antibody were purchased from Santa Cruz Biotechnology (Dallas, USA).

2.2. Cell culture

Human neuroblastoma SH-SY5Y cells were cultured in DMEM supplemented with 10% FBS and 1% penicillin and streptomycin. Acetaldehyde was diluted in PBS and added to the cell culture medium to achieve specific concentrations. The cells were maintained at 37 °C in a humidified atmosphere with 5% CO2 and 95% air until being collected for different assays.

2.3. MTT assay

SH-SY5Y cells were seeded at a density of 4×10^3 cells/well in a 96-well culture plate. Primary cultures of cortical neurons prepared from the brains of newborn Sprague/Dawley rats were seeded with a density of 2×10^3/well in growth neurobasal medium containing 2% B27 and 1% FBS. Cells were treated with various concentrations of acetaldehyde. After the treatment, MTT solution was added to each well and the cells were incubated at 37 °C for 4 h. The medium was then discarded and the cells were incubated at 37 °C for 15 min in 150 μL DMSO to dissolve the formazan. The colored products were then measured at 570 nm using a microplate reader.

2.4. Determination of mitochondrial membrane potential

The mitochondrial membrane potential was measured using an assay kit following the manufacturer's protocol. After the treatment, cells were incubated at 37 °C for 20 min with a JC-1 working buffer. Cells were washed twice and harvested by trypsinization. The fluorescence intensity of the cells was then measured using a fluorospectrophotometer (F-2700 Techcomp (China) Ltd.) (excitation wavelength: 490 nm; emission wavelength: 590 and 525 nm). The relative mitochondrial membrane potential was estimated using the ratio of red/green fluorescence intensity.

2.5. Measurement of ATP content

The ATP content was measured using a luciferase luminescent ATP detection assay kit, according to the manufacturer's instructions. After the treatment, cells were lysed with a lysis buffer provided by the manufacturer and centrifuged at 12,000 × *g* at 4 °C for 10 min. The supernatants or ATP standard solutions with known concentrations were mixed with luciferin and luciferase. Luciferase converted luciferin to oxyluciferin and light, which is proportional to the concentration of ATP present in the reaction mixture. The luminescence was measured using a Synergy HTX Multi-mode Microplate Reader (Biotek Instruments, Inc.). Then the concentration of ATP was calculated according to the standard curve.

2.6. Analyses of mitochondrial morphology

The morphology of mitochondria was examined using MitoTracker Green staining. Cells were seeded in a 29 mm glass bottom dish (Cellvis, Mountain View, CA, USA). After treatment, cells were fixed with 4% paraformaldehyde at room temperature for 15 min, washed twice with FBS-free medium, and stained with MitoTracker Green (180 nM) at 37 °C for 30 min in the dark. Mitochondrial morphology was then examined using a confocal laser scanning microscope (FluoView FV1000) (60 × objective, zoom × 2). The excitation/emission wavelengths for MitoTracker Green FM were 490/516 nm. Images were analyzed using Image-Pro Plus 6.0 software. Approximately 45–60 cells were randomly chosen from each treatment. The mitochondrial morphology were analyzed using three different parameters, length, aspect ratio (AR) (ratio between major and minor axes of an ellipse) and form factor (FF) (perimeter^2/4π·area; degree of branching) according to previous studies [34,35]. Average values of AR and FF were calculated from each experiment. Individual mitochondria were sub-divided into three categories according to their lengths: fragmented (< 1.2 μm), intermediate (1.2–1.6 μm), and tubular (> 1.6 μm). A total of three parallel treatments were counted and the experiment was repeated three times.

2.7. Mitochondria isolation

Mitochondria were prepared using a mitochondria isolation kit following the manufacturer's instructions. Briefly, approximately 1×10^7 cells were harvested and centrifuged at 700 × *g* for 10 min at 4 °C, the pellets were then suspended with 500 μL isolation buffer provided by the manufacture. The cells were homogenized on ice for 60 strokes using a pestle and then centrifuged at 3500 × *g* for 25 min at 4 °C. The pellets were used as mitochondrial fraction. The supernatant was collected and centrifuged at 12,000 × *g* for 10 min at 4 °C, and the resulted supernatant was used as cytosolic fraction.

2.8. Western blot analyses

After treatments, cells were washed twice with PBS and lysed in a lysis buffer (Tris 20 mM, NaCl 150 mM, EDTA 1 mM, sodium pyrophosphate 2.5 mM, NaF 20 mM, β-glycerophosphoric acid 1 mM, and sodium orthovanadate 1 mM). The supernatants were collected after centrifugation at 14,000 × *g* for 10 min at 4 °C. 20 μg of protein extracts was resolved by SDS-polyacrylamide gel electrophoresis and then transferred to polyvinylidene difluoride (PVDF) membrane and subsequently incubated with specific primary antibodies. PVDF membrane was washed by Tris buffered saline (TBS) containing 0.1% Tween-20 for three times. For detection, the PVDF membrane was incubated with a horseradish peroxidase-coupled secondary antibody, followed by an enhanced chemiluminescence substrate reaction using BeyoECL plus Western blotting detection system.

2.9. Measurement of ROS levels

The conversion of non-fluorescent DCFH-DA to fluorescent dichlorofluorescein (DCF) was used to monitor the intracellular ROS production as described previously [36] with minor modifications. In brief, cells were seeded in 6-well culture plates. After treatment, the cells were washed with PBS and harvested by trypsinization. The cells were then stained with 10 μM DCFH-DA for 30 min at 37 °C in the dark. The cells were then washed with PBS and the fluorescence intensity was analyzed immediately using a Synergy HTX Multi-mode Microplate Reader (excitation at 488 nm, emission at 525 nm).

The detection of mitochondrial ROS was performed as described previously [37] with minor modifications. Cells were co-stained with MitoSOX Red and MitoTracker Green. After treatment, cells were stained with MitoSOX Red mitochondrial superoxide indicator (5 μM) diluted in DMEM with 10% FBS at 37 °C for 15 min, and washed with PBS for three times. Cells were then stained with MitoTracker Green (180 nM) diluted in FBS-free DMEM at 37 °C for 30 min. Cells were washed by PBS and the mitochondrial ROS production was evaluated using an Olympus BX53 fluorescence microscope (excitation at 480–550 nm, emission at 590 nm).

2.10. Ca^{2+} measurement

The levels of Ca^{2+} in SH-SY5Y cells were measured using Fluo-3 AM as described previously [38] with minor modifications. After treatment, cells were washed by PBS twice, and incubated with 2.5 μM Fluo-3 AM in FBS-free medium at 37 °C for 40 min in the dark. The cells were then washed twice by PBS and incubated at 37 °C for additional 30 min. Cells were collected by trypsinization and the fluorescence intensity was measured using a Synergy HTX Multi-mode Microplate Reader with excitation at 488 nm and emission at 525 nm.

2.11. Statistical analysis

Statistical analyses of the data were performed by one-way or two-way ANOVA. Least significant difference (LSD) test was used for pairwise comparisons. $P < 0.05$ was considered statistically significant.

3. Results

3.1. Acetaldehyde induces cytotoxicity and impairs mitochondrial function

Acetaldehyde treatment has been shown to induce cytotoxicity in primary neuronal cells and SH-SY5Y cells [29,[31]]. As shown in Fig. 1A and B, MTT assay showed that acetaldehyde treatment for 24 h induced toxicity in both rat cortical neurons and SH-SY5Y cells in a dose-dependent manner. It was also found that acetaldehyde induced toxicity of SH-SY5Y cells as early as 2 h after treatment (Fig. 1C). When crystal violet assay was performed to estimate the cell viability, no significant cell loss was detected under these experimental conditions (Fig. S1). The MTT assay measures the reduction of MTT to formazan by succinate dehydrogenase (SDH) in complex II of the electron transport chain and reflects the activity of mitochondria [39,40,42]. Therefore, the results from MTT assays suggested that the damage of mitochondrial function might be an earlier event in acetaldehyde-induced cytotoxicity. We then examined the effects of acetaldehyde on mitochondrial membrane potential, which is an indicator for mitochondrial integrity and bioenergetics function [43]. As shown in Fig. 1D, treatment with 100 μM and 500 μM acetaldehyde for 24 h reduced the mitochondrial membrane potential of SH-SY5Y cells by approximately 34% and 42%, respectively. The decrease of mitochondrial membrane potential was observed as early as 1 h after acetaldehyde treatment (Fig. 1E). Disruption of mitochondrial membrane potential has been shown to disturb proton gradient and lead to the loss of ATP production [44]. Consistently, our data showed that the production of ATP in SH-SY5Y cells was significantly decreased by acetaldehyde treatment (Fig. 1F and G). These results indicated that impairment of mitochondrial function was an early event in acetaldehyde-induced cytotoxicity.

It was noted that the reduction of MTT activity by acetaldehyde treatment was smaller in comparison with the decrease of mitochondrial membrane potential or the loss of ATP production. The MTT activity reflects predominantly the activity of SDH, which is an important mitochondrial metabolic enzyme. It was possible that compensatory mechanisms existed to prevent the decrease of the activity of SDH in response to acetaldehyde-induced ATP loss and mitochondrial damages, thus resulting in a less dramatic decrease of MTT activity. However, this assumption has yet to be proved.

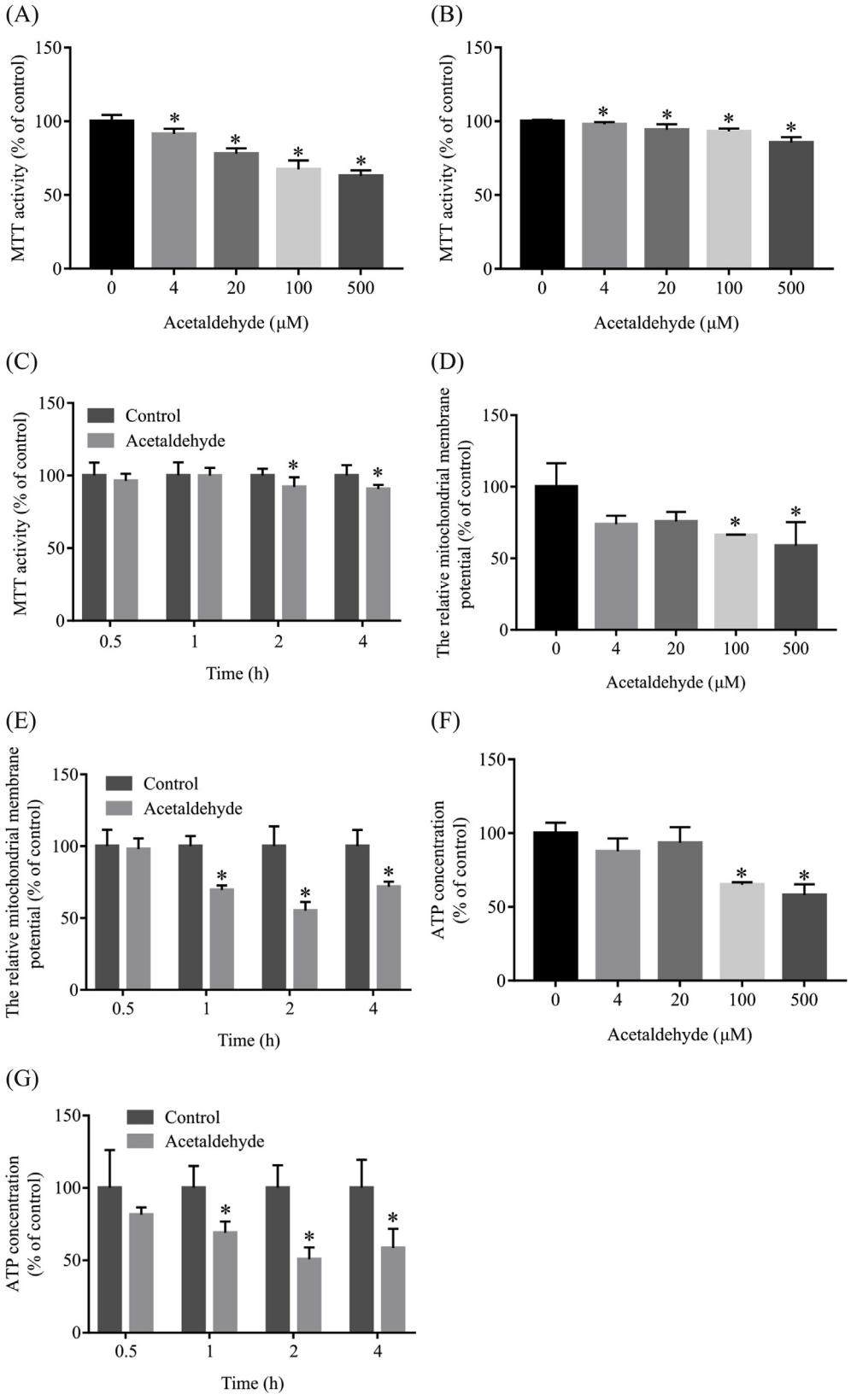

Fig. 1. Acetaldehyde induces cytotoxicity and impairs mitochondrial function. Primary cultures of cortical neurons **(A)** or SH-SY5Y cells **(B, D and F)** were exposed to various concentrations of acetaldehyde (0, 4, 20, 100, 500 μM) for 24 h, or exposed to 500 μM acetaldehyde for the indicated period of time **(C, E and G)**. After the treatment, MTT assay **(A, B, and C)**, JC-1 mitochondrial membrane potential assay **(D, E)** or ATP luminescent detection assay **(F, G)** was performed. Data represent mean ± SEM, n = 6 **(A, B and C)** or n = 3 **(D, E, F and G)**. *$p < 0.05$ versus control.

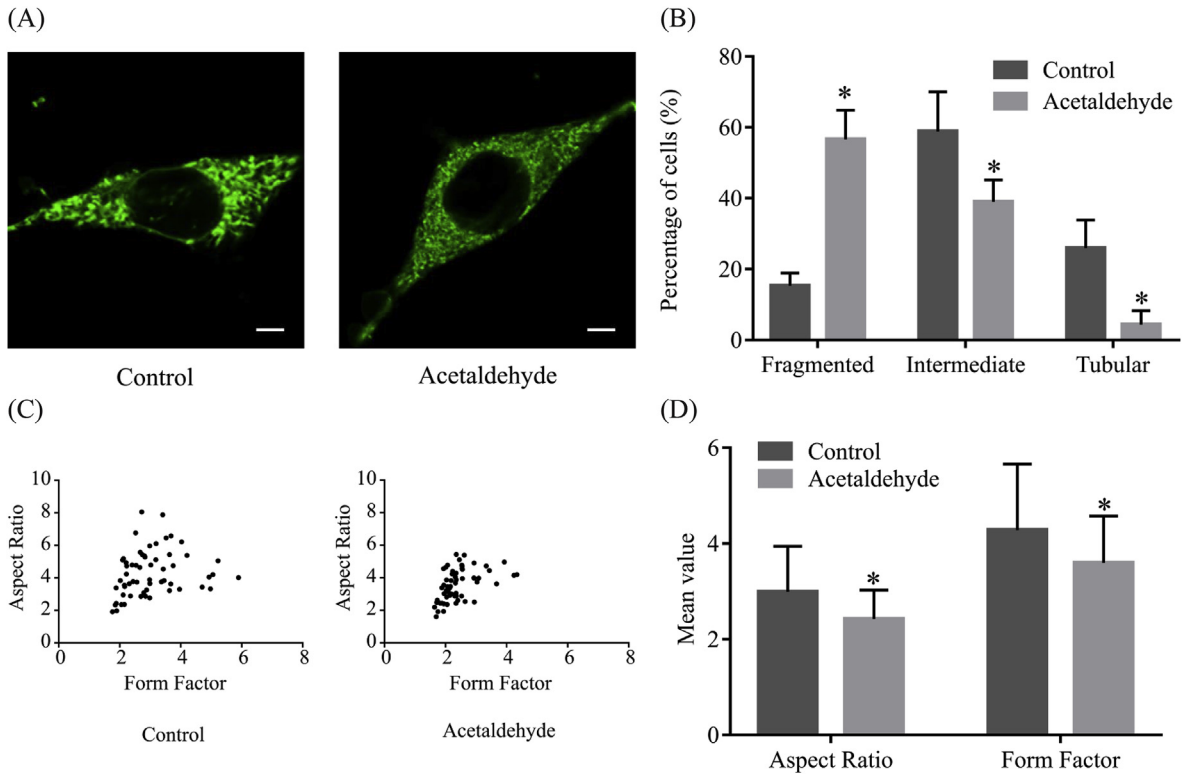

Fig. 2. Acetaldehyde induces abnormal mitochondrial morphology of SH-SY5Y cells. (A) SH-SY5Y cells were exposed to acetaldehyde (500 μM) for 24 h. Cells were stained with MitoTracker Green and examined by a laser confocal microscope. Data are representative images from three independent experiments. Scale bar, 5 μm. **(B)** The percentages of cells with fragmented, intermediated and tubular mitochondria after control or acetaldehyde-treatment. Data represent mean ± SEM, n = 3. **(C)** Representative Scattered plots and **(D)** the average values of aspect ratio and form factor of control and acetaldehyde-treated cells (n = 3). The data shown are representative of three independent experiments with similar results. *p < 0.05 versus control. (For interpretation of the references to color in this figure legend, the reader is referred to the Web version of this article.)

3.2. Effects of acetaldehyde on mitochondrial morphology and key fission/fusion proteins

Normal structure and morphology are essential for the function of mitochondria [5,12]. The effect of acetaldehyde on mitochondrial morphology was then evaluated by MitoTracker Green staining. As shown in Fig. 2A, in cells treated with acetaldehyde, the mitochondria had shorter and rounder shapes with less mitochondrial network continuity. Specifically, in comparison with the control-treated cells, the number of cells with fragmented shape (< 1.2 μm) was increased by approximately 2.7 folds, while the number of cells with intermediate (1.2–1.6 μm) and tubular shape (> 1.6 μm) was decreased by approximately 34% and 83%, respectively, after treatment with acetaldehyde (Fig. 2B). When the values of AR and FF were calculated, it was found that AR and FF were decreased by about 19% and 16%, respectively (Fig. 2C and D), suggesting that the mitochondria in acetaldehyde-treated cells were rounder and more fragmented.

Mitochondrial fragmentation can be caused by excessive fission and/or fusion deficiency [45–47]. A wide variety of proteins are involved in the regulation of mitochondrial dynamics. The fusion of the outer and the inner membrane of mitochondria is mediated by dynamin-related GTPases mitofusin (Mfn) and optic atrophy 1 (Opa1), respectively [48]. As shown in Fig. 3, the protein levels of Mfn1 and OPA1 were not significantly affected by acetaldehyde treatment. The fission of mitochondria is mainly mediated by GTPase dynamic-related protein Drp1 [49,50]. Excessive phosphorylation of Drp1 at Ser616 induces mitochondrial fragmentation and dysfunction in multiple pathological processes while inhibition of Drp1 phosphorylation at Ser616 attenuates mitochondrial damage [51–53]. As shown in Fig. 4A and B, though the protein levels of Drp1 were not significantly affected by acetaldehyde treatment, a dramatic increase of Drp1 phosphorylation at Ser616 was detected as early as 2 h after acetaldehyde treatment. The levels of p-Drp1 (Ser616) in cells treated with 500 μM acetaldehyde for 2 h were about 2-folds of that in the control cells. Further analyses of the levels of Drp1 proteins in mitochondrial and cytoplasmic fraction of the cells showed that acetaldehyde treatment promoted the translocation of p-Drp1 (Ser616) to mitochondria (Fig. 4C). Thus, the elevation of Drp1 phosphorylation and its translocation to mitochondria might be a major mechanism that caused mitochondrial fragmentation in acetaldehyde-treated SH-SY5Y cells.

3.3. Elevated ROS production and MAPK activation are critical for acetaldehyde-induced cytotoxicity and Drp1 phosphorylation

Acetaldehyde has been shown to induce oxidative stress in neuronal cells [29,31]. As shown in Fig. 5A, exposure of acetaldehyde caused a quick increase in the production of intracellular ROS in SH-SY5Y cells in a dose-response manner. The levels of ROS were increased by approximately 27% and 69% in cells treated with 100 μM and 500 μM acetaldehyde in comparison to that of the control cells, respectively. As expected, pretreatment with NAC, a well-known antioxidant, significantly attenuated the elevation of intracellular ROS production induced by acetaldehyde (Fig. 5B). Mitochondria are believed to be the major source of intracellular ROS [2]. To elucidate the source of the ROS production in acetaldehyde-treated cells, we next measured the production of mitochondrial ROS by co-staining the cells with MitoSOX Red and MitoTracker Green. As shown in Fig. 5C, acetaldehyde treatment elevated the ROS levels in the mitochondria of SH-SY5Y cells, while pretreatment of NAC inhibited acetaldehyde-induced generation of ROS in mitochondria.

The elevation of ROS appeared to play an important role in acetaldehyde-induced mitochondrial dysfunction and cytotoxicity, as NAC

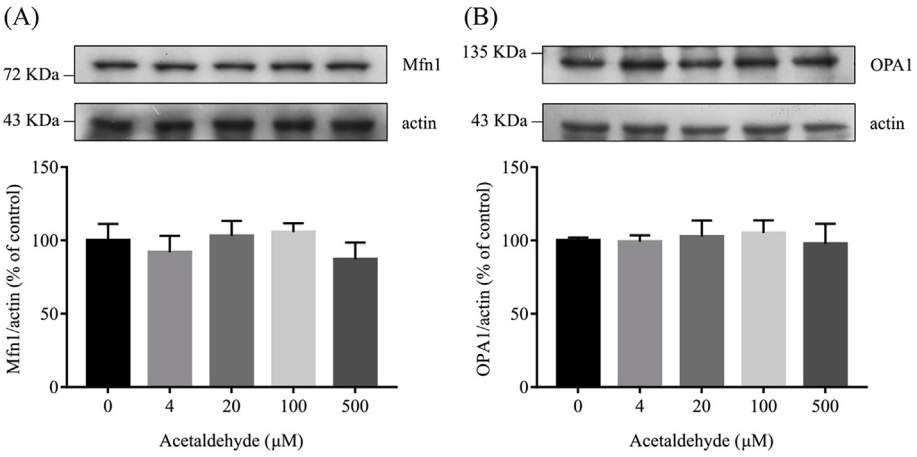

Fig. 3. Effects of acetaldehyde on mitochondrial fusion-related proteins in SH-SY5Y cells. SH-SY5Y cells were exposed to various concentrations of acetaldehyde (0, 4, 20, 100, 500 μM) for 24 h. The protein levels of Mfn1 and OPA1 in the cell lysates were determined by Western blot analyses. The intensities of the bands were quantified by densitometric analyses and normalized by the amount of actin. Data represent the mean ± SEM of 3 independent experiments.

pretreatment significantly alleviated acetaldehyde-induced suppression of cell activity (Fig. 5D). As shown in Fig. 5E, NAC pretreatment also significantly inhibited acetaldehyde-induced Drp1 phosphorylation, suggesting that ROS-mediated cell signaling was essential for acetaldehyde-induced phosphorylation of Drp1 and mitochondrial fragmentation.

JNK and p38 MAPK are important downstream mediators of ROS in the pathophysiological process of neurodegeneration [55,56]. As shown in Fig. 6A and B, acetaldehyde treatment increased the levels of activated JNK and p38 MAPK by approximately 100% and 66%, respectively, while pretreatment with NAC blocked the activation of JNK and p38 MAPK, almost restoring it to the similar levels of those in untreated cells. It has been demonstrated that activated MAPKs promotes Drp1 phosphorylation at Ser616 [57]. To find out whether the activation of JNK or p38 MAPK mediates acetaldehyde-induced phosphorylation of Drp1 at Ser616, cells were pretreated with sp600125, the inhibitor of JNK, or sb203580, the inhibitor of p38 MAPK, before acetaldehyde treatment. As shown in Fig. 6C and D, acetaldehyde-induced excessive phosphorylation of Drp1 at Ser616 was dramatically attenuated by pretreatment with sp600125 or sb203580. These results suggested that the phosphorylation of Drp1 at Ser616 induced by acetaldehyde was at least partly dependent on the activation of JNK and p38 MAPK; and JNK and p38 MAPK might be important downstream effectors of ROS in acetaldehyde-induced Drp1 phosphorylation and cytotoxicity.

3.4. Ca^{2+}-mediated signaling is involved in acetaldehyde-induced cytotoxicity and Drp1 phosphorylation in SH-SY5Y cells

Previous studies have demonstrated that Ca^{2+} influx evokes mitochondrial dysfunction and fragmentation [58,59]. As shown in Fig. 7A and B, acetaldehyde treatment significantly elevated the levels of intracellular Ca^{2+}. At 2 h after acetaldehyde (500 μM) treatment, the

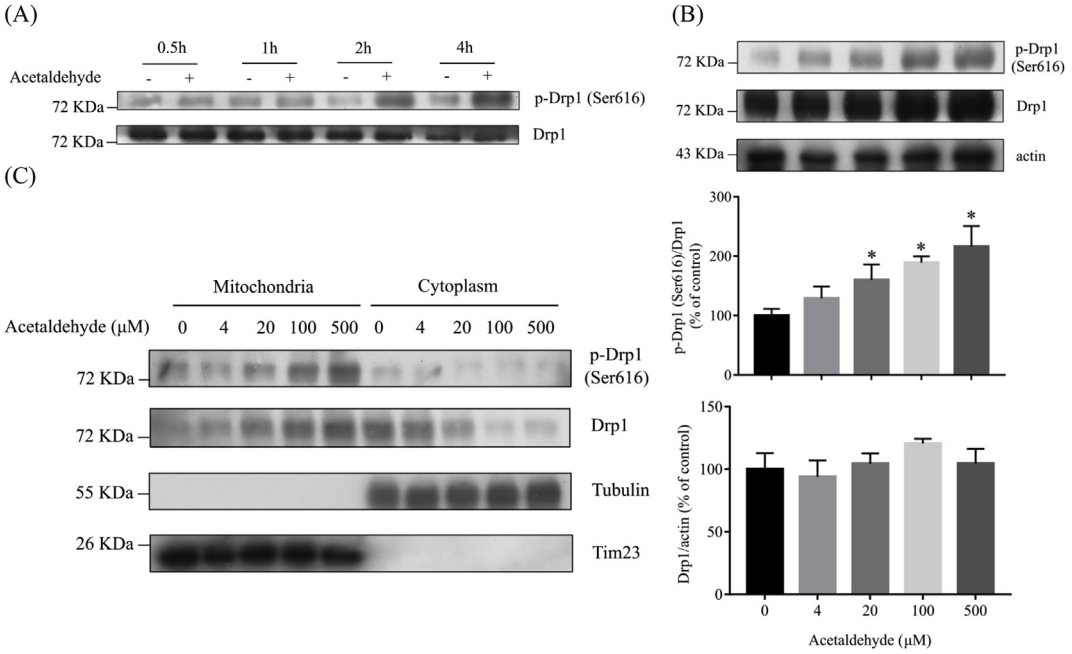

Fig. 4. Acetaldehyde promotes Drp1 phosphorylation at Ser616 and the translocation of Drp1 to mitochondria. SH-SY5Y cells were exposed to acetaldehyde (500 μM) for the indicated period of time **(A)** or at various concentrations (0, 4, 20, 100, 500 μM) for 2 h **(B)**. Whole cell lysates were prepared and the protein levels of p-Drp1 (Ser616) and Drp1 were determined by Western blot analyses. **(C)** SH-SY5Y cells were exposed to acetaldehyde at various concentrations (0, 4, 20, 100, 500 μM) for 24 h. The mitochondrial and cytoplasmic fractions were prepared and the protein levels of p-Drp1 (Ser616) and Drp1 were determined by Western blot analyses. Tubulin and Tim23 were used as internal control of cytoplasm and mitochondria, respectively. The intensities of the bands were quantified by densitometric analyses and normalized by the amount of Drp1 or actin as indicated in the graphs. Data represent the mean ± SEM of 3 independent experiments. *p < 0.05 versus control.

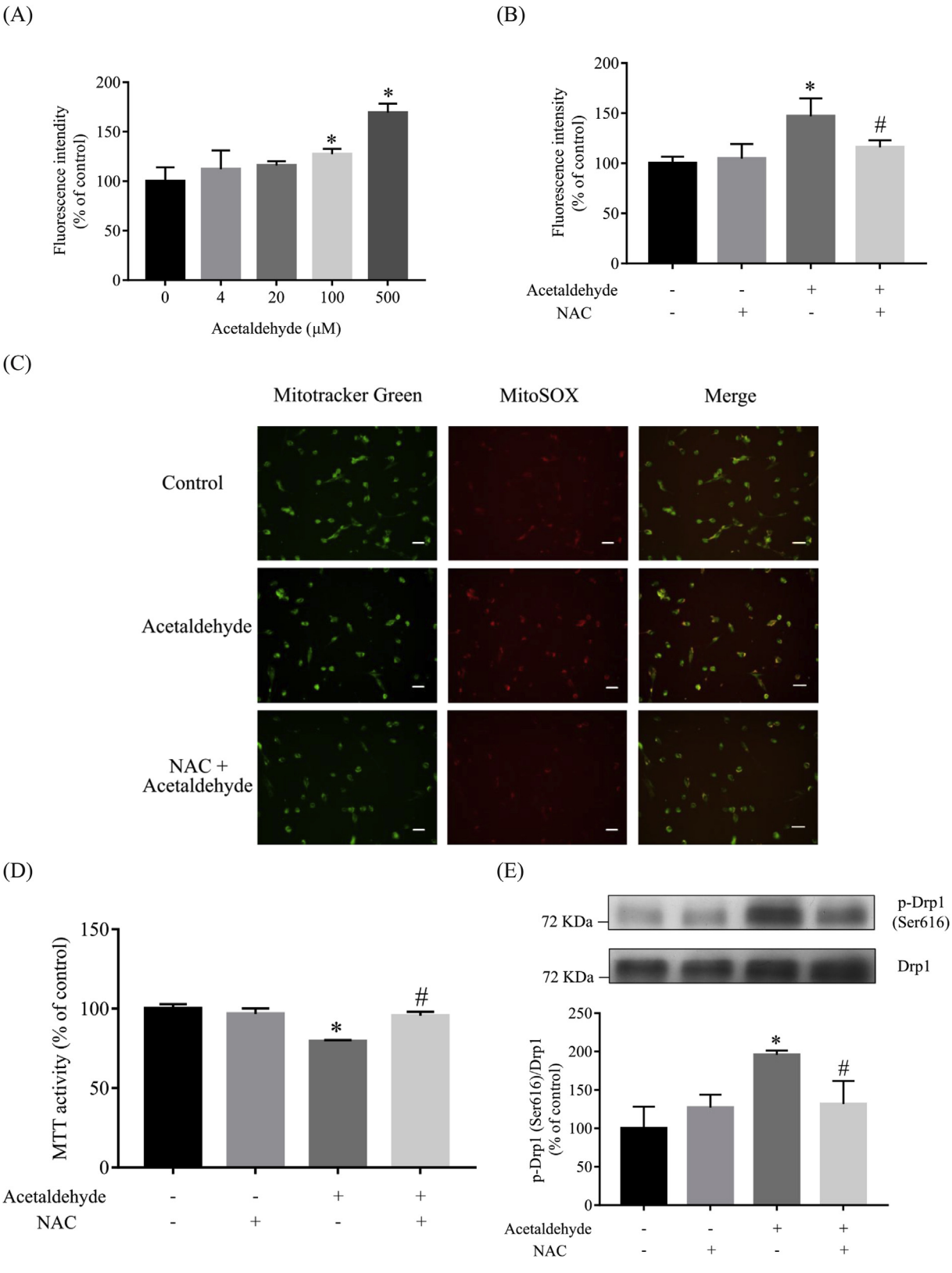

(caption on next page)

levels of intracellular Ca^{2+} were increased by approximately 50% in comparison with the control. To find out whether the elevation of intracellular Ca^{2+} is essential for acetaldehyde-induced Drp1 phosphorylation, cells were pretreated with BAPTA-AM, a permeable free Ca^{2+} chelator. As shown in Fig. 7C, pretreatment with BAPTA-AM ameliorated acetaldehyde-induced increase of Drp1 phosphorylation. CaMKII is a downstream effector of Ca^{2+} influx [60]. Acetaldehyde treatment triggered the activation of CaMKII by increasing the phosphorylation of CaMKII at Thr286, while pretreatment with BAPTA-AM prevented its activation induced by acetaldehyde treatment (Fig. 7D).

Fig. 5. Acetaldehyde-induced ROS production is critical for acetaldehyde-induced cytotoxicity and Drp1 phosphorylation. (A) SH-SY5Y cells were treated with various concentrations of acetaldehyde (0, 4, 20, 100, 500 μM) for 0.5 h. **(B)** SH-SY5Y cells preincubated with NAC (1 mM) for 1 h were treated with acetaldehyde (500 μM) for 0.5 h. ROS production was determined by DCFH-DA staining as described in "Materials and Methods". **(C)** SH-SY5Y cells preincubated with NAC (1 mM) for 1 h were treated with acetaldehyde (500 μM) for 0.5 h. The cells were co-stained with MitoSOX Red and MitoTracker Green, and examined with a fluorescence microscope. Data are representative images of three independent experiments with similar results. Scale bar, 60 μm. **(D)** SH-SY5Y cells preincubated with NAC (1 mM) for 1 h were treated with acetaldehyde (500 μM) for 24 h. The MTT assay was then performed. **(E)** SH-SY5Y cells preincubated with NAC (1 mM) for 1 h were treated with acetaldehyde (500 μM) for 2 h. The protein levels of p-Drp1 (Ser616) were determined in whole cell lysates by Western blot analyses. The intensities of the bands were quantified by densitometric analyses and normalized by the amount of Drp1. Data represent the mean ± SEM of 3 independent experiments. *$p < 0.05$ versus control; #$p < 0.05$ versus acetaldehyde-treated group. (For interpretation of the references to color in this figure legend, the reader is referred to the Web version of this article.)

To explore the role of CaMKII in acetaldehyde-induced mitochondrial dysfunction and cytotoxicity, cells were preincubated with CaMKII inhibitor KN-93 before acetaldehyde treatment. MTT assay showed that KN-93 significantly attenuated acetaldehyde-induced cytotoxicity (Fig. 7E). Moreover, KN-93 pretreatment prevented acetaldehyde-induced increase of Drp1 phosphorylation at Ser616 (Fig. 7F). These results suggested that Ca^{2+}-mediated signaling pathways might play key roles in acetaldehyde-induced mitochondrial fragmentation and cytotoxicity.

Evidence suggests that ROS can induce CaMKII phosphorylation at Thr286 [61,62]. When the effect of NAC on the phosphorylation of CaMKII at Thr286 was examined in cells treated with acetaldehyde, it was found that pretreatment with NAC significantly ameliorated acetaldehyde-induced CaMKII phosphorylation (Fig. 7G). Besides, pretreatment with NAC dramatically inhibited the increase of intracellular Ca^{2+} levels induced by acetaldehyde (Fig. 7H), suggesting that acetaldehyde-induced ROS production might promote cellular events that led to Ca^{2+} influx.

4. Discussion

Acetaldehyde, the most toxic metabolite of ethanol, has been demonstrated to induce mitochondrial damages and cause cytotoxicity [29,[31,32],], but the detailed mechanisms remain unknown. In this study, it was found that acetaldehyde treatment elevated Drp1 phosphorylation, induced mitochondrial fragmentation and impaired mitochondrial function.

The normal mitochondrial morphology and function are maintained by a variety of proteins that regulate the equilibrium of mitochondrial fission and fusion processes. Alteration of these regulatory proteins leads to reduction of mitochondrial fusion or excessive mitochondrial fission, causing mitochondrial fragmentation and the formation of small

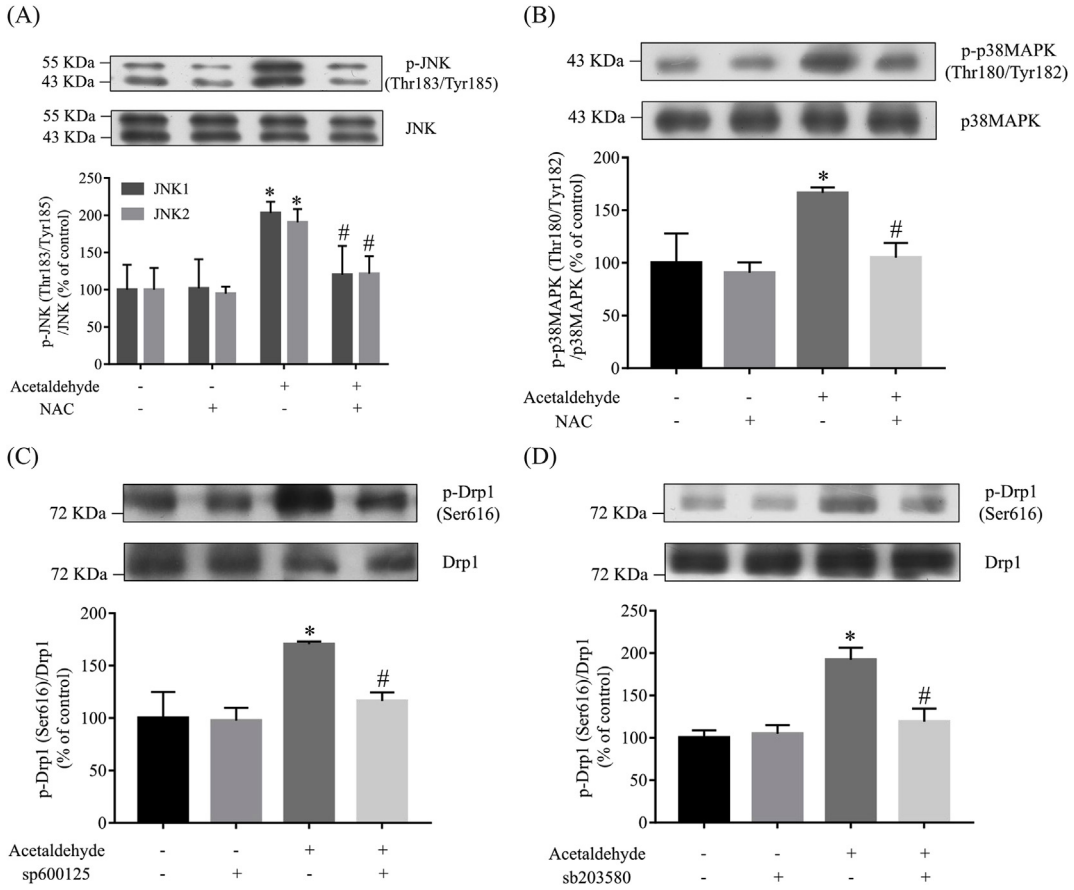

Fig. 6. ROS-mediated activation of JNK and p38 MAPK is important for Drp1 phosphorylation induced by acetaldehyde. SH-SY5Y cells preincubated with NAC (1 mM) for 1 h were treated with acetaldehyde (500 μM) for 2 h. The levels of p-JNK (Thr183/Tyr185) **(A)** and p-p38MAPK (Thr180/Tyr182) **(B)** were determined by Western blot analyses. **(C)** SH-SY5Y cells were preincubated with sp600125 (20 μM) or sb203580 (5 μM) **(D)** for 0.5 h, then treated with acetaldehyde (500 μM) for 2 h. The levels of p-Drp1 (Ser616) were determined by Western blot analyses. The intensities of the bands were quantified by densitometric analyses and normalized by the amount of JNK, p38MAPK or Drp1. Data represent the mean ± SEM of 3 independent experiments. *$p < 0.05$ versus control; #$p < 0.05$ versus acetaldehyde-treated group.

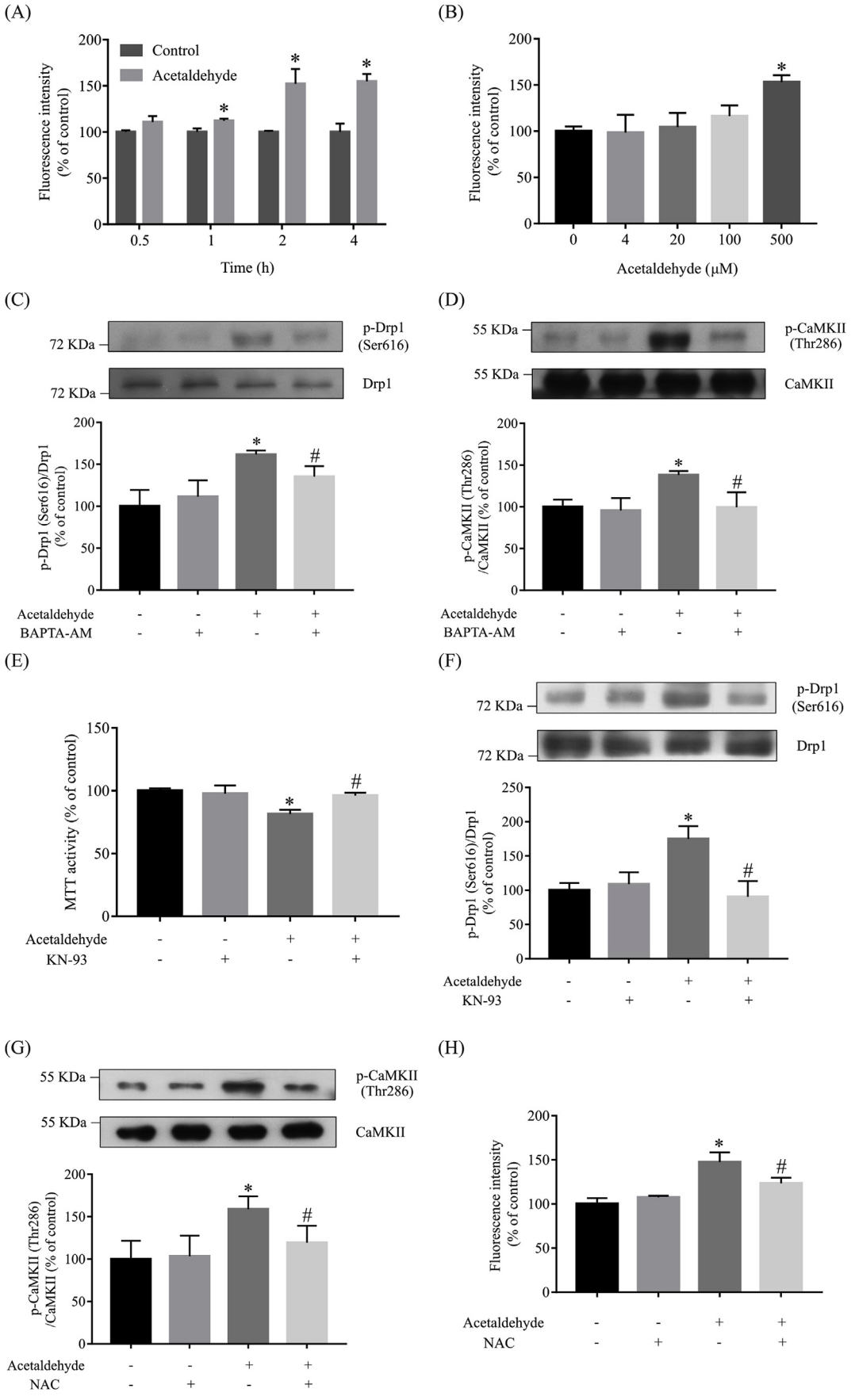

(caption on next page)

Fig. 7. Ca^{2+}-mediated signaling is involved in acetaldehyde-induced cytotoxicity and Drp1 phosphorylation in SH-SY5Y cells. SH-SY5Y cells were treated with acetaldehyde (500 μM) for the indicated period of time **(A)** or various concentrations (0, 4, 20, 100, 500 μM) for 24 h **(B)**. Cells were stained with Fluo-3 AM to determine the intracellular Ca^{2+} concentration. SH-SY5Y cells preincubated with BAPTA-AM (10 μM) for 0.5 h were treated with acetaldehyde (500 μM) for 2 h. Protein levels of p-Drp1 (Ser616) **(C)** and p-CaMKII (Thr286) **(D)** were determined by Western blot analyses. **(E)** SH-SY5Y cells preincubated with KN-93 (1 μM) for 1 h were treated with acetaldehyde (500 μM) for 24 h. MTT assay were then performed. **(F)** SH-SY5Y cells preincubated with KN-93 (1 μM) for 1 h were treated with acetaldehyde (500 μM) for 2 h. Protein levels of p-Drp1 (Ser616) were determined by Western blot analyses. **(G)** SH-SY5Y cells preincubated with NAC (1 mM) for 1 h were treated with acetaldehyde (500 μM) for 2 h. Protein levels of p-CaMKII (Thr286) were determined by Western blot analyses. Intracellular Ca^{2+} concentration was analyzed by staining cells with Fluo-3 AM **(H)**. The intensities of the bands on Western blots were quantified by densitometric analyses and normalized by the amount of Drp1 or CaMKII. Data represent the mean ± SEM of 3 independent experiments. *$p < 0.05$ versus control, #$p < 0.05$ versus acetaldehyde-treated group.

round defective mitochondria [63–66]. It was found that the levels of mitochondrial fusion and fission related proteins, Mfn1, OPA1 and Drp1, were not significantly affected by acetaldehyde treatment. However, the phosphorylation of Drp1 at Ser616 was significantly increased in acetaldehyde-treated cells. Drp1 is regulated by various posttranslational modifications, among which phosphorylation has been extensively studied [67,68]. Phosphorylation of Drp1 at Ser616 promotes both the localization of Drp1 to mitochondria and its assembly into large oligomeric structures at mitochondrial fission sites, which are important for initiating the fission event [17–19]. Consistently, it was observed that Drp1 was translocated from cytoplasm to mitochondria after acetaldehyde treatment, in accordance with the increased number of rounder and more fragmented mitochondria as well as the reduced mitochondrial membrane potential and the loss of ATP production. Thus, the induction of Drp1 phosphorylation at Ser616 and the subsequent excessive mitochondrial fission are important mechanisms by which acetaldehyde causes mitochondrial dysfunction.

Mitochondrial electron transport chain is the major source of intracellular ROS; when the mitochondrial respiratory chain complex is damaged, ROS can be overproduced and accumulated, causing oxidative stress [2,69] and triggering more mitochondrial alterations (e.g., ΔΨm disruption and ATP depletion) [70]. Studies have shown that acetaldehyde targets mitochondria, elevating mitochondrial ROS formation and causing oxidative stress in various cell and animal models [27,28,71,72]. Consistently, our results also showed that acetaldehyde treatment increased the ROS generation in mitochondria of SH-SY5Y cells. Moreover, prevention of oxidative stress by antioxidant NAC reduced acetaldehyde-induced Drp1 phosphorylation at Ser616 while ameliorating the cytotoxicity induced by acetaldehyde, suggesting that the oxidative stress triggered by acetaldehyde was a key factor that mediated mitochondrial fragmentation and cytotoxicity. The data also suggested that inhibition of oxidative stress by antioxidant might be an effective way to intervene the cytotoxicity induced by acetaldehyde.

ROS triggered activation of JNK and p38 MAPK has been demonstrated to contribute to the pathophysiological process of neurodegeneration induced by mitochondrial defects [55,56]. It has been shown that the activation of JNK or p38 MAPK is involved in the phosphorylation of Drp1 at Ser616 [57]. Furthermore, p38 MAPK could directly phosphorylate cytosolic Drp1 at Ser616, promoting the translocation of Drp1 to mitochondrial outer membrane and inducing mitochondrial fragmentation [73]. Our data demonstrated that JNK and p38 MAPK might be important downstream signals of ROS that led to Drp1 phosphorylation at Ser616 in acetaldehyde-treated cells.

Moreover, our data showed that Ca^{2+} influx and Ca^{2+}-mediated signaling cascades contributed to acetaldehyde-induced Drp1 phosphorylation. Acetaldehyde treatment induced a quick entry of Ca^{2+} into cells, while prevention of the elevation of intracellular Ca^{2+} levels attenuated the phosphorylation of Drp1. The elevated intracellular Ca^{2+} levels activate a variety of Ca^{2+}-dependent protein kinases and phosphatases, including CaMKII [74,75]. It is reported that activated CaMKII can directly bind and phosphorylate Drp1 at Ser616, leading to excessive mitochondrial fission and mitochondrial fragmentation [52]. Our results demonstrated that acetaldehyde induced the activation of CaMKII, while pretreatment of cells with CaMKII specific inhibitor KN-93 ameliorated acetaldehyde-induced phosphorylation of Drp1 at Ser616. Thus, CaMKII was activated in acetaldehyde treated cells upon Ca^{2+} influx and subsequently mediated the phosphorylation of Drp1, causing mitochondrial fragmentation and dysfunction.

It has to be noted that acetaldehyde-induced CaMKII phosphorylation at Thr286 could be inhibited by NAC. Previous studies have demonstrated that ROS can activate CaMKII in Ca^{2+} dependent [76] or independent manner [77]. Therefore, both Ca^{2+} overload and ROS elevation could contribute to CaMKII activation in acetaldehyde-treated cells, though the precise mechanisms remain to be established. Furthermore, it was found that NAC treatment effectively inhibited the Ca^{2+} influx triggered by acetaldehyde treatment, suggesting that acetaldehyde-induced oxidative stress might promote cellular events that lead to calcium influx. Indeed, there are multiple lines of evidence that ROS can trigger the elevation of intracellular Ca^{2+} levels through modulating Ca^{2+} sensors and transporters located on ER, mitochondria or plasma membrane [78,80]. Conversely, Ca^{2+} overload can lead to dysregulation of mitochondrial Ca^{2+} that increases ROS generation by enhancing metabolic pathways favoring ROS production which can further damage Ca^{2+} transport mechanisms [81–83]. Thus, a positive feedback loop exists between ROS generation and Ca^{2+} influx, which may play an important role in acetaldehyde-induced mitochondrial dysfunction and cytotoxicity. It appears that CaMKII is a key component in the crosstalk of Ca^{2+} and ROS-mediated signaling cascades, which mediates the phosphorylation of Drp1 at Ser616 and the consequent mitochondrial fragmentation in cells treated with acetaldehyde.

In summary, acetaldehyde treatment induced oxidative stress and Ca^{2+} overload in SH-SY5Y cells, leading to the phosphorylation of Drp1 at Ser616 and the translocation of Drp1 to mitochondria, subsequently causing excessive fission and fragmentation of mitochondria (Fig. 8). The resulted imbalance of mitochondrial dynamics eventually impaired mitochondrial function and caused cytotoxicity. As a key modulator of mitochondrial dynamics, Drp1 plays a crucial role in determining the destiny of neurons in neurodegenerative diseases such as AD, PD and Huntington's disease [20,84–88]. Therefore, acetaldehyde-induced Drp1 activation and mitochondrial fragmentation may contribute to the promotion of AD pathogenesis by alcohol abuse. Meanwhile, inhibition of oxidative stress by antioxidant may be beneficial for preventing neuronal damages associated with alcohol abuse by preserving the normal morphology and function of mitochondria.

Funding

This work was supported by the National Natural Science Foundation of China [31371082], research fund from Harbin Institute of Technology at Weihai [HIT(WH)Y200902] and Weihai Science and Technology Development Program [2009-3-93 and 2011DXGJ14].

Declaration of competing interest

None.

Appendix A. Supplementary data

Supplementary data to this article can be found online at https://doi.org/10.1016/j.redox.2019.101381.

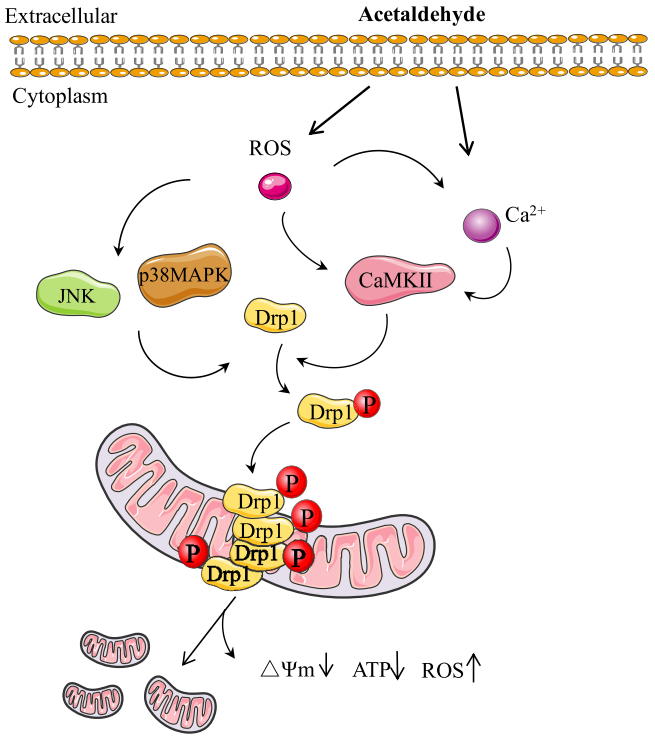

Fig. 8. Acetaldehyde may induce mitochondrial dysfunction through ROS and Ca^{2+}-mediated signaling pathways.

References

[1] O. Kann, R. Kovács, Mitochondria and neuronal activity, Am. J. Physiol. Cell Physiol. 292 (2007) C641–C657, https://doi.org/10.1152/ajpcell.00222.2006.

[2] N. Apostolova, V.M. Victor, Molecular strategies for targeting antioxidants to mitochondria: therapeutic implications, Antioxidants Redox Signal. 22 (2015) 686–729, https://doi.org/10.1089/ars.2014.5952.

[3] M. Pera, D. Larrea, C. Guardialaguarta, et al., Increased localization of APP-C99 in mitochondria-associated ER membranes causes mitochondrial dysfunction in Alzheimer disease, EMBO J. 36 (2017) 3356–3371, https://doi.org/10.15252/embj.201796797.

[4] X.L. Wang, B. Su, H. Lee, et al., Impaired balance of mitochondria fission and fusion in Alzheimer disease, J. Neurosci. 29 (2009) 9090–9103, https://doi.org/10.1523/JNEUROSCI.1357-09.2009.

[5] T. Ishihara, R. Ban-Ishihara, M. Maeda, et al., Dynamics of mitochondrial DNA nucleoids regulated by mitochondrial fission is essential for maintenance of homogeneously active mitochondria during neonatal heart development, Mol. Cell. Biol. 35 (2015) 211–223, https://doi.org/10.1128/MCB.01054-14.

[6] E. Bossy-wetzel, M.J. Barsoum, A. Godzik, et al., Mitochondrial fission in apoptosis, neurodegeneration and aging, Curr. Opin. Cell Biol. 15 (2003) 706–716, https://doi.org/10.1016/j.ceb.2003.10.015.

[7] B. Duboff, M. Feany, J. Götz, Why size matters-balancing mitochondrial dynamics in Alzheimer's disease, Trends Neurosci. 36 (2013) 325–335, https://doi.org/10.1016/j.tins.2013.03.002.

[8] K. Hirai, G. Aliev, A. Nunomura, et al., Mitochondrial abnormalities in Alzheimer's disease, J. Neurosci. 21 (2001) 3017–3023, https://doi.org/10.1523/JNEUROSCI.21-09-03017.2001.

[9] M.J. Calkins, M. Manczak, P. Mao, et al., Impaired mitochondrial biogenesis, defective axonal transport of mitochondria, abnormal mitochondrial dynamics and synaptic degeneration in a mouse model of Alzheimer's disease, Hum. Mol. Genet. 20 (2011) 4515–4529, https://doi.org/10.1093/hmg/ddr381.

[10] X.L. Wang, B. Su, S.L. Siedlak, et al., Amyloid-beta overproduction causes abnormal mitochondrial dynamics via differential modulation of mitochondrial fission/fusion proteins, P Natl Acad Sci USA 105 (2008) 19318–19323, https://doi.org/10.1073/pnas.0804871105.

[11] L. Tilokani, S. Nagashima, V. Paupe, et al., Mitochondrial dynamics: overview of molecular mechanisms, Essays Biochem. 62 (2018) 341–360, https://doi.org/10.1042/EBC20170104.

[12] H. Chen, A. Chomyn, D.C. Chan, Disruption of fusion results in mitochondrial heterogeneity and dysfunction, J. Biol. Chem. 280 (2005) 26185–26192, https://doi.org/10.1074/jbc.M503062200.

[13] B. Lu, B. Kennedy, R.W. Clinton, et al., Steric interference from intrinsically disordered regions controls dynamin-related protein 1 self-assembly during mitochondrial fission, Sci. Rep. 8 (2018) 10879, , https://doi.org/10.1038/s41598-018-29001-9.

[14] R. Kalia, R.Y.R. Wang, A. Yusuf, et al., Structural basis of mitochondrial receptor binding and constriction by DRP1, Nature 558 (2018) 401–405, https://doi.org/10.1038/s41586-018-0211-2.

[15] H. Otera, N. Ishihara, K. Mihara, New insights into the function and regulation of mitochondrial fission, Biochim. Biophys. Acta 1833 (2013) 1256–1268, https://doi.org/10.1016/j.bbamcr.2013.02.002.

[16] F.C. Luo, K. Herrup, X. Qi, et al., Inhibition of Drp1 hyper-activation is protective in animal models of experimental multiple sclerosis, Exp. Neurol. 292 (2017) 21–34, https://doi.org/10.1016/j.expneurol.2017.02.015.

[17] A.M.V.D. Bliek, Q.F. Shen, S. Kawajiri, Mechanisms of mitochondrial fission and fusion, Cold Spring Harb Perspect Biol 5 (2013) a011072, , https://doi.org/10.1101/cshperspect.a011072.

[18] A.R. Hall, N. Burke, R.K. Dongworth, et al., Mitochondrial fusion and fission proteins: novel therapeutic targets for combating cardiovascular disease, Br. J. Pharmacol. 171 (2014) 1890–1906, https://doi.org/10.1111/bph.12516.

[19] B. Ugarte-Uribe, C. Prévost, K.K. Das, et al., Drp1 polymerization stabilizes curved tubular membranes similar to those of constricted mitochondria, J. Cell Sci. 132 (2018), https://doi.org/10.1242/jcs.208603.

[20] B. Kim, J. Park, K.T. Chang, et al., Peroxiredoxin 5 prevents amyloid-beta oligomer-induced neuronal cell death by inhibiting ERK-Drp1-mediated mitochondrial fragmentation, Free Radical Biol. Med. 90 (2015) 184–194, https://doi.org/10.1016/j.freeradbiomed.2015.11.015.

[21] C.H.L. Hung, S.S.Y. Cheng, Y.T. Cheung, et al., A reciprocal relationship between reactive oxygen species and mitochondrial dynamics in neurodegeneration, Redox Bio 14 (2017) 7–19, https://doi.org/10.1016/j.redox.2017.08.010.

[22] S. Xu, H. Pi, Y. Chen, et al., Cadmium induced Drp1-dependent mitochondrial fragmentation by disturbing calcium homeostasis in its hepatotoxicity, Cell Death Dis. 4 (2013) e540, , https://doi.org/10.1038/cddis.2013.7.

[23] G.T. Sutherland, D. Sheedy, J.J. Kril, Using autopsy brain tissue to study alcohol-related brain damage in the genomic age, Alcohol Clin. Exp. Res. 38 (2014) 1–8, https://doi.org/10.1111/acer.12243.

[24] J.Y. Yang, X. Xue, H. Tian, et al., Role of microglia in ethanol-induced neurodegenerative disease: pathological and behavioral dysfunction at different developmental stages, Pharmacol. Ther. 144 (2014) 321–337, https://doi.org/10.1016/j.pharmthera.2014.07.002.

[25] D.W. Crabb, S. Liangpunsakul, Acetaldehyde generating enzyme systems: roles of alcohol dehydrogenase, CYP2E1 and catalase, and speculations on the role of other enzymes and processes, Novartis Found. Symp. 285 (2007) 4–16, https://doi.org/10.1002/9780470511848.ch2 discussion 16-22, 198-9.

[26] G.S. Peng, S.J. Yin, Effect of the allelic variants of aldehyde dehydrogenase ALDH2*2 and alcohol dehydrogenase ADH1B*2 on blood acetaldehyde concentrations, Hum. Genom. 3 (2009) 121–127, https://doi.org/10.1186/1479-7364-3-2-121.

[27] M. Tamura, H. Ito, H. Matsui, et al., Acetaldehyde is an oxidative stressor for gastric epithelial cells, J. Clin. Biochem. Nutr. 55 (2014) 26–31, https://doi.org/10.3164/jcbn.14-12.

[28] P. Wenzel, J. Müller, S. Zurmeyer, et al., ALDH-2 deficiency increases cardiovascular oxidative stress-evidence for indirect antioxidative properties, Biochem Bioph Res Co 367 (2008) 137–143, https://doi.org/10.1016/j.bbrc.2007.12.089.

[29] T.T. Yan, Y. Zhao, X. Zhang, et al., Astaxanthin inhibits acetaldehyde- induced cytotoxicity in SH-SY5Y cells by modulating Akt/CREB and p38MAPK/ERK signaling pathways, Mar. Drugs 14 (2016) 56–68, https://doi.org/10.3390/md14030056.

[30] M. Brandt, V. Garlapati, M. Oelze, et al., NOX2 amplifies acetaldehyde mediated cardiomyocyte mitochondrial dysfunction in alcoholic cardiomyopathy, Sci. Rep. 6 (2016) 32554, , https://doi.org/10.1038/srep32554.

[31] J. Haorah, S.H. Ramirez, N. Floreani, et al., Mechanism of alcohol-induced oxidative stress and neuronal injury, Free Radic. Biol. Med. 45 (2008) 1542–1550, https://doi.org/10.1016/j.freeradbiomed.2008.08.030.

[32] J. Haorah, N.A. Floreani, B. Knipe, et al., Stabilization of superoxide dismutase by acetyl-l-carnitine in human brain endothelium during alcohol exposure: novel protective approach, Free Radical Biol. Med. 51 (2011) 1601–1609, https://doi.org/10.1016/j.freeradbiomed.2011.06.020.

[34] T. Yu, J.L. Robotham, Y. Yoon, Increased production of reactive oxygen species in hyperglycemic conditions requires dynamic change of mitochondrial morphology, P Natl Acad Sci USA 103 (2006) 2653–2658, https://doi.org/10.1073/pnas.0511154103.

[35] P. Theurey, E. Tubbs, G. Vial, et al., Mitochondria-associated endoplasmic reticulum membranes allow adaptation of mitochondrial metabolism to glucose availability in the liver, J. Mol. Cell Biol. 8 (2016) 129–143, https://doi.org/10.1093/jmcb/mjw004.

[36] B.M. Emerling, J.B. Hurov, G. Poulogiannis, et al., Depletion of a putatively druggable class of phosphatidylinositol kinases inhibits growth of p53-null tumors, Cell 155 (2013) 844–857, https://doi.org/10.1016/j.cell.2013.09.057.

[37] J.L. Larson Casey, J.S. Deshane, A.J. Ryan, et al., Macrophage Akt1 kinase-mediated mitophagy modulates apoptosis resistance and pulmonary fibrosis, Immunity 44 (2016) 582–596, https://doi.org/10.1016/j.immuni.2016.01.001.

[38] X.T. Lin, Y. Zhao, S.H. Li, Astaxanthin attenuates glutamate-induced apoptosis via inhibition of calcium influx and endoplasmic reticulum stress, Eur. J. Pharmacol. 806 (2017) 43–51, https://doi.org/10.1016/j.ejphar.2017.04.008.

[39] Y. Rai, R. Pathak, N. Kumari, et al., Mitochondrial biogenesis and metabolic hyperactivation limits the application of MTT assay in the estimation of radiation induced growth inhibition, Sci. Rep. 8 (2018) 1531–1545, https://doi.org/10.1038/s41598-018-19930-w.

[40] I. Kaneko, N. Yamada, Y. Sakuraba, et al., Suppression of mitochondrial succinate dehydrogenase, a primary target of β-amyloid, and its derivative racemized at ser residue, J. Neurochem. 65 (1995) 2585–2593, https://doi.org/10.1046/j.1471-

4159.1995.65062585.x.
[41] K.Y. Kim, G.A. Perkins, M.S. Shim, et al., DRP1 inhibition rescues retinal ganglion cells and their axons by preserving mitochondrial integrity in a mouse model of glaucoma, Cell Death Dis. 6 (2015) e1839, , https://doi.org/10.1038/cddis.2015.180.
[42] K. Abe, H. Saito, Amyloid β protein inhibits cellular MTT reduction not by suppression of mitochondrial succinate dehydrogenase but by acceleration of MTT formazan exocytosis in cultured rat cortical astrocytes, Neurosci. Res. 31 (1998) 295–305, https://doi.org/10.1016/S0168-0102(98)00055-8.
[43] J. Nunnari, A. Suomalainen, Mitochondria: in sickness and in health, Cell 148 (2012) 1145–1159, https://doi.org/10.1016/j.cell.2012.02.035.
[44] S.P. Soltoff, Rottlerin: an inappropriate and ineffective inhibitor of PKCδ, Trends Pharmacol. Sci. 28 (2007) 453–458, https://doi.org/10.1016/j.tips.2007.07.003.
[45] J. Vowinckel, J. Hartl, R. Butler, et al., MitoLoc: a method for the simultaneous quantification of mitochondrial network morphology and membrane potential in single cells, Mitochondrion 24 (2015) 77–86, https://doi.org/10.1016/j.mito.2015.07.001.
[46] Y.C. Su, H.W. Chiu, J.C. Hung, et al., Beta-nodavirus B2 protein induces hydrogen peroxide production, leading to Drp1-recruited mitochondrial fragmentation and cell death via mitochondrial targeting, Apoptosis 19 (2014) 1457–1470, https://doi.org/10.1007/s10495-014-1016-x.
[47] G. Goyal, B. Fell, A. Sarin, et al., Role of mitochondrial remodeling in programmed cell death in drosophila melanogaster, Dev. Cell 12 (2007) 807–816, https://doi.org/10.1016/j.devcel.2007.02.002.
[48] V. Parra, H.E. Verdejo, M. Iglewski, et al., Insulin stimulates mitochondrial fusion and function in cardiomyocytes via the Akt-mTOR-NFκB-Opa-1 signaling pathway, Diabetes 63 (2014) 75–88, https://doi.org/10.2337/db13-0340.
[49] B.M. Michalska, K. Kwapiszewska, J. Szczepanowska, et al., Insight into the fission mechanism by quantitative characterization of Drp1 protein distribution in the living cell, Sci. Rep. 8 (2018) 8122–8137, https://doi.org/10.1038/s41598-018-26578-z.
[50] J.A. Kashatus, A. Nascimento, L.J. Myers, et al., Erk2 phosphorylation of Drp1 promotes mitochondrial fission and MAPK-driven tumor growth, Mol. Cell 57 (2015) 537–551, https://doi.org/10.1016/j.molcel.2015.01.002.
[51] S. Kumari, S.L. Mehta, G.Z. Milledge, et al., Ubisol-Q10 prevents glutamate-induced cell death by blocking mitochondrial fragmentation and permeability transition pore opening, Int. J. Biol. Sci. 12 (2016) 688–700, https://doi.org/10.7150/ijbs.13589.
[52] S.C. Xu, P. Wang, H.L. Zhang, et al., CaMKII induces permeability transition through Drp1 phosphorylation during chronic β-AR stimulation, Nat. Commun. 7 (2016) 13189, , https://doi.org/10.1038/ncomms13189.
[53] X. Qi, M.H. Disatnik, N. Shen, et al., Aberrant mitochondrial fission in neurons induced by protein kinase Cδ under oxidative stress conditions in vivo, Mol. Biol. Cell 22 (2011) 256–265, https://doi.org/10.1007/s11064-015-1788-6.
[55] L. Liu, K. Zhang, H. Sandoval, et al., Glial lipid droplets and ROS induced by mitochondrial defects promote neurodegeneration, Cell 160 (2015) 177–190, https://doi.org/10.1016/j.cell.2014.12.019.
[56] V. Debattisti, A.A. Gerencser, M. Saotome, et al., ROS control mitochondrial motility through p38 and the motor adaptor miro/trak, Cell Rep. 21 (2017) 1667–1680, https://doi.org/10.1016/j.celrep.2017.10.060.
[57] J.H. Park, J. Ko, J. Hwang, et al., Dynamin-related protein 1 mediates mitochondria-dependent apoptosis in chlorpyrifos-treated SH-SY5Y cells, Neurotoxicology (Little Rock) 51 (2015) 145–157, https://doi.org/10.1016/j.neuro.2015.10.008.
[58] X.J. Han, Y.F. Lu, S.A. Li, et al., CaM kinase Iα-induced phosphorylation of Drp1 regulates mitochondrial morphology, J. Cell Biol. 182 (2008) 573–585, https://doi.org/10.1083/jcb.200802164.
[59] C.D. SanMartín, P. Veloso, T. Adasme, et al., RyR2-mediated Ca^{2+} release and mitochondrial ROS generation partake in the synaptic dysfunction caused by Amyloid β peptide oligomers, Front. Mol. Neurosci. 10 (2017) 115–131, https://doi.org/10.3389/fnmol.2017.00115.
[60] M.B. Kennedy, Signal-processing machines at the postsynaptic density, Science 290 (2000) 750–754, https://doi.org/10.1126/science.290.5492.750.
[61] S.S. Jain, S. Paglialunga, C. Vigna, et al., High-fat diet-induced mitochondrial biogenesis is regulated by mitochondrial-derived reactive oxygen species activation of CaMKII, Diabetes 63 (2014) 1907–1913, https://doi.org/10.2337/db13-0816.
[62] K.V. Premkumar, S.K. Chaube, Increased level of reactive oxygen species persuades postovulatory aging-mediated spontaneous egg activation in rat eggs cultured in vitro, Vitro Cell Dev-An 52 (2016) 576–588, https://doi.org/10.1007/s11626-016-0007-3.
[63] B. Duboff, J. Götz, M.B. Feany, Tau promotes neurodegeneration via DRP1 mislocalization in vivo, Neuron 75 (2012) 618–632, https://doi.org/10.1016/j.neuron.2012.06.026.
[64] M. Song, K. Mihara, Y. Chen, et al., Mitochondrial fission and fusion factors reciprocally orchestrate mitophagic culling in mouse hearts and cultured fibroblasts, Cell Metabol. 21 (2015) 273–285, https://doi.org/10.1016/j.cmet.2014.12.011.
[65] R. Chandra, M. Engeln, C. Schiefer, et al., Drp1 mitochondrial fission in D1 neurons mediates behavioral and cellular plasticity during early cocaine abstinence, Neuron 96 (2017) 1327–1341, https://doi.org/10.1016/j.neuron.2017.11.037 e6.
[66] D. Sebastián, M. Palacín, A. Zorzano, Mitochondrial dynamics: coupling mitochondrial fitness with healthy aging, Trends Mol. Med. 23 (2017) 201–215, https://doi.org/10.1016/j.molmed.2017.01.003.
[67] W.B. Jang, J.H. Park, S.T. Ji, et al., Cytoprotective roles of a novel compound, MHY-1684, against hyperglycemia-induced oxidative stress and mitochondrial dysfunction in human cardiac progenitor cells, Oxid Med Cell Longev 2018 (2018) 4528184, , https://doi.org/10.1155/2018/4528184.
[68] D.G. Lee, J.S. Min, H.S. Lee, et al., Isoliquiritigenin attenuates glutamate- induced mitochondrial fission via calcineurin-mediated Drp1 dephosphorylation in HT22 hippocampal neuron cells, Neurotoxicology (Little Rock) 68 (2018) 133–141, https://doi.org/10.1016/j.neuro.2018.07.011.
[69] G. Arena, M.Y. Cisse, S. Pyrdziak, et al., Mitochondrial MDM2 regulates respiratory complex I activity independently of p53, Mol. Cell 69 (2018) 594–609, https://doi.org/10.1016/j.molcel.2018.01.023.
[70] W.J. Heuett, V. Periwal, Autoregulation of free radicals via uncoupling protein control in pancreatic β-cell mitochondria, Biophys. J. 98 (2010) 207–217, https://doi.org/10.1016/j.bpj.2009.10.012.
[71] D. Clavijo-cornejo, M. Gutiérrez-carrera, M. Palestino-domínguez, et al., Acetaldehyde targets superoxide dismutase 2 in liver cancer cells inducing transient enzyme impairment and a rapid transcriptional recovery, Food Chem. Toxicol. 69 (2014) 102–108, https://doi.org/10.1016/j.fct.2014.04.002.
[72] M. Dezest, M.L. Bechec, L. Chavatte, et al., Oxidative damage and impairment of protein quality control systems in keratinocytes exposed to a volatile organic compounds cocktail, Sci. Rep. 7 (2017) 10707, , https://doi.org/10.1038/s41598-017-11088-1.
[73] S.H. Ko, G.E. Choi, J.Y. Oh, et al., Succinate promotes stem cell migration through the GPR91-dependent regulation of DRP1-mediated mitochondrial fission, Sci. Rep. 7 (2017) 12582, , https://doi.org/10.1038/s41598-017-12692-x.
[74] M. Land, C.S. Rubin, A calcium- and diacylglycerol-stimulated protein kinase C (PKC), caenorhabditis elegans PKC-2, links thermal signals to learned behavior by acting in sensory neurons and intestinal cells, Mol. Cell. Biol. 37 (2017), https://doi.org/10.1128/MCB.00192-17 e00192-17.
[75] C. Hong, H. Seo, M. Kwak, et al., Increased TRPC5 glutathionylation contributes to striatal neuron loss in Huntington's disease, Brain 138 (2015) 3030–3047, https://doi.org/10.1093/brain/awv188.
[76] S. Wagner, H.M. Ruff, S.L. Weber, et al., ROS-activated Ca/calmodulin kinase IIδ is required for late INa augmentation leading to cellular Na and Ca overload, Circ. Res. 108 (2011) 555–565, https://doi.org/10.1161/CIRCRESAHA.110.221911.
[77] J. Palomeque, O.V. Rueda, L. Sapia, et al., Angiotensin II-induced oxidative stress resets the Ca^{2+} dependence of Ca^{2+}-calmodulin protein kinase II and promotes a death pathway conserved across different species, Circ. Res. 105 (2009) 1204–1212, https://doi.org/10.1161/CIRCRESAHA.109.204172.
[78] D.M. Booth, S.K. Joseph, G. Hajnóczky, Subcellular ROS imaging methods: relevance for the study of calcium signaling, Cell Calcium 60 (2016) 65–73, https://doi.org/10.1016/j.ceca.2016.05.001.
[79] X.L. Wang, B. Su, L. Zheng, et al., The role of abnormal mitochondrial dynamics in the pathogenesis of Alzheimer's disease, J. Neurochem. 109 (2009) 153–159, https://doi.org/10.1111/j.1471-4159.2009.05867.x.
[80] G. Csordás, G. Hajnóczky, SR/ER-mitochondrial local communication: calcium and ROS, Biochim. Biophys. Acta 1787 (2009) 1352–1362, https://doi.org/10.1016/j.bbabio.2009.06.004.
[81] R.G. Hansford, D. Zorov, Role of mitochondrial calcium transport in the control of substrate oxidation, Mol. Cell. Biochem. 184 (1998) 359–369, https://doi.org/10.1023/A:1006893903113.
[82] Y. Han, S. Ishibashi, J. Iglesiasgonzalez, et al., Ca^{2+}-induced mitochondrial ROS regulate the early embryonic cell cycle, Cell Rep. 22 (2018) 218–231, https://doi.org/10.1016/j.celrep.2017.12.042.
[83] J. Ouchi, S.Y. Ryu, B.S. Jhun, et al., Mitochondrial ion channels/transporters as sensors and regulators of cellular redox signaling, Antioxidants Redox Signal. 21 (2014) 987–1006, https://doi.org/10.1089/ars.2013.5681.
[84] J. Yan, X.H. Liu, M.Z. Han, et al., Blockage of GSK3β-mediated Drp1 phosphorylation provides neuroprotection in neuronal and mouse models of Alzheimer's disease, Neurobiol. Aging 36 (2015) 211–227, https://doi.org/10.1016/j.neurobiolaging.2014.08.005.
[85] M.J. Calkins, P.H. Reddy, Amyloid beta impairs mitochondrial anterograde transport and degenerates synapses in Alzheimer's disease neurons, Biochim. Biophys. Acta 1812 (2011) 507–513, https://doi.org/10.1016/j.bbadis.2011.01.007.
[86] N. Xie, C. Wang, Y. Lian, et al., Inhibition of mitochondrial fission attenuates Aβ-induced microglia apoptosis, Neuroscience 256 (2014) 36–42, https://doi.org/10.1016/j.neuroscience.2013.10.011.
[87] F. Zhao, W.Z. Wang, C.Y. Wang, et al., Mfn2 protects dopaminergic neurons exposed to paraquat both in vitro and in vivo: implications for idiopathic Parkinson's disease, Biochim. Biophys. Acta 1863 (2017) 1359–1370, https://doi.org/10.1016/j.bbadis.2017.02.016.
[88] W.J. Song, J. Chen, A. Petrilli, et al., Mutant huntingtin binds the mitochondrial fission GTPase dynamin-related protein-1 and increases its enzymatic activity, Nat. Med. 17 (2011) 377–382, https://doi.org/10.1038/nm.2313.